Presented at the 32th JANNAF Combustion Meeting, Huntsville, Alabama, October, 1995.

Comparison of the Thermal Decompositions of HMX and 2,4-DNI for Evaluation of Slow Cookoff Response and Long-Term Stability

Leanna Minier and Richard Behrens‡
Combustion Research Facility
Sandia National Laboratories
Livermore, CA 94551

Suryanarayana Bulusu*
Energetic Materials Division
U.S. Army Armament Research, Development, and Engineering Center
Dover, NJ 07801-5001

ABSTRACT

The thermal decomposition of HMX between 175°C and 200°C has been studied using the simultaneous thermogravimetric modulated beam mass spectrometer (STMBMS) apparatus with a focus on the initial stages of the decomposition. The identity of thermal decomposition products is the same as that measured in previous higher temperature experiments. The initial stages of the decomposition are characterized by an induction period followed by two acceleratory periods. The Arrhenius parameters for the induction and two acceleratory periods are (Log(A)= 18.2 ± 0.8, Ea = 48.2 ± 1.8 kcal/mole), (Log (A) = 17.15 ± 1.5 and Ea = 48.9 ± 3.2 kcal/mole), (Log (A) = 19.1 ± 3.0 and Ea = 52.1 ± 6.3 kcal/mole), respectively. This data can be used to calculate the time and temperature required to decompose a desired fraction of a test sample that is being prepared to test the effect of thermal degradation on its sensitivity or burn rates. It can also be used to estimate the extent of decomposition that may be expected under normal storage conditions for munitions containing HMX. This data, along with previous mechanistic studies conducted at higher temperatures, suggest that the process that controls the early stages of decomposition of HMX in the solid phase is scission of the N-NO_2 bond, reaction of the NO_2 within a "lattice cage" to form the mononitroso analogue of HMX and decomposition of the mononitroso HMX within the HMX lattice to form gaseous products that are retained in bubbles or diffuse into the surrounding lattice. These methods evaluating HMX can be used to evaluate new energetic materials such as 2,4-DNI. The early 2,4-DNI thermal decomposition is characterized by an initial decomposition, an apparent induction period, then an initial acceleratory period. The main gaseous products are NO, CO_2, HNCO, H_2O, N_2, CO, HCN and C_2N_2. The presence of adsorbed and occluded H_2O is the major cause of the early decomposition. The Arrhenius parameters for the induction period are [Log(A) = 16.3 ± 0.3 and Ea = 46.9 ± 0.7 kcal/mole] and for the initial accelerating period are [Log (A) = 13.4 ± 1.7 and Ea = 42.7 ± 3.9 kcal/mole]. Thus, our data shows that the thermal stabilities of both materials at nominal temperatures extend to a large number of years and that 2,4-DNI stability exceeds that of HMX.

INTRODUCTION

Understanding the thermal decomposition of HMX (I) is important for developing models to predict the response of munitions in abnormal thermal environments and to obtain an understanding of the chemical processes that control its long-term degradation.

The objective of this work is threefold. First, we seek to develop a model that can be used to estimate the extent of thermal decomposition of HMX as a function of time and temperature. This model can be used to guide experiments that are aimed at determining the response of degraded explosives or propellants that contain HMX. For example, high pressure burn rate measurements of thermally degraded HMX formulations are currently being carried out at LLNL[1] and this information should help guide the degradation of the test samples prior to initiation of combustion. Second, we wish to ascertain the extent and characteristics of decomposition that may occur at lower temperatures which could affect the long-term aging of components containing HMX. In this work the rates of thermal decomposition at lower temperatures will be measured and insight into the processes that control the decomposition of HMX will be developed. Third, in light of the new insensitive energetic materials being

‡ Work supported by a memorandum of understanding between the U.S. Department of Energy and the office of munitions and by the U.S. Department of Energy under contract DE-AC04-94AL8530.
* Work supported by the U. S. Army, ARDEC.

developed, we wish to assess the low-temperature thermal decomposition of one such material, 2,4-dinitroimidazole (2,4-DNI; II), and compare it to that of HMX.

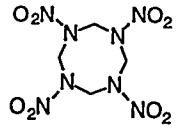

I

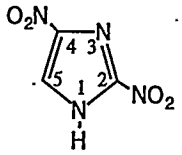

II

The work presented in this report is an extension of our previous work on the thermal decomposition of cyclic nitramines, in particular HMX, to lower temperatures and recent work on the thermal decomposition of 2,4-DNI.

INSTRUMENTATION AND METHODS

A description of the STMBMS apparatus and the experimental procedures that are used in this study have been previously described in detail.[2,3] For this study, samples on the order of 10 mg are pyrolyzed. Using the described method, we have previously conducted extensive studies on the thermal decomposition of HMX[3] and RDX[4,5] in an effort to determine the reaction mechanisms that control the decomposition of these two cyclic nitramines.

HMX THERMAL DECOMPOSITION PROCESS

PREVIOUS RESULTS

For RDX in the liquid phase (m.p. 200°C), the identities of the gaseous products and their rates of formation have been identified and from these results a reaction mechanism consisting of four parallel reaction pathways were found to control the decomposition of RDX in the liquid phase. Details of the RDX decomposition mechanism have been published.[4,5] In the solid phase, RDX was found to decompose through intermediate that is the mononitroso analogue of RDX, hexahydro-1-nitroso-3,5-dinitro-s-triazine (ONDNTA).

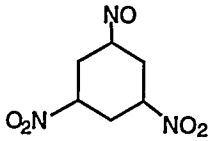

ONDNTA

In contrast to RDX, HMX liquefies between 270° and 280°C and undergoes substantial decomposition in the solid phase. The identity and rates of formation of the products formed in the thermal decomposition of HMX have been determined and a qualitative model describing the process has been developed.[6] The thermal decomposition process of HMX is illustrated with the data shown in Figure 1. The main decomposition products are H_2O, N_2O, CH_2O, NO and CO. The temporal behavior of the gas formation rates of each of the products is characterized by the following sequence: 1) an induction period, 2) an increasing rate of formation between 0 and 10% decomposition, 3) a faster rate of decomposition between 10% and 30% decomposition and a decreasing rate of gas formation after 40% decomposition. Products formed at smaller rates of formation but with similar temporal behaviors include: $(CH_3)_2NNO$, the mononitroso analogue of HMX (1-nitroso-3,5,7-trinitro-1,3,5,7-tetrazocene) and several formamides. The temporal behavior of the decomposition process during the induction period is illustrated with data from the decomposition of a deuterium labeled analogue of HMX, as shown in Figure 2. From this figure one observes a period of time in which the rates of formation of N_2O and CD_2O are low and constant with time. The time at which the gas formation rates first reach a constant value coincides with attaining an isothermal temperature of 235°C in the sample. The time period between the time that the isothermal temperature is reached and when the N_2O signal first starts to increase is referred to as the induction period. The gas formation rates of N_2O and CH_2O during the induction period arise from the decomposition of HMX in either the gas phase or on the surface of the particles.

During the induction period of HMX the material is somehow transformed to a new state that undergoes more rapid decomposition. This transformation could be a nucleation process as observed in the decomposition of many inorganic salts in which nuclei are formed and destroyed while those that reach a certain critical diameter form the basis for the accelerating rate of decomposition as the nuclei grow. The transformation may also be due to the slow decomposition of the HMX within the lattice and the permeation of its gaseous products through the crystal structure, weakening the crystal structure, and leading to the release of gaseous products and the more rapid decomposition of noncrystalline material. This latter mechanism is consistent with the observation of the mononitroso analogue of RDX in the decomposition of RDX in the solid phase and the delay time observed for the onset of rapid decomposition during its decomposition as discussed in a previous paper.[7] It is important to note that

the HMX must be undergoing some significant change during the induction period. The acceleratory phase of the decomposition process marks a transition to a more rapid decomposition process. During this phase the HMX undergoes a more rapid rate of decomposition.

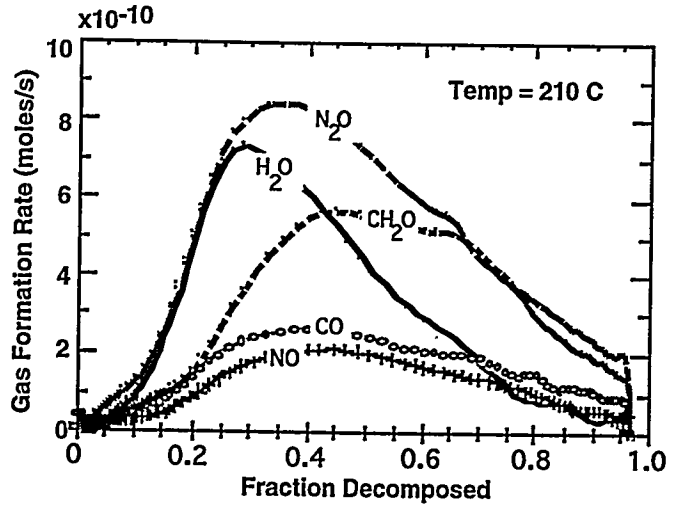

Figure 1. Gas formation rates of the products from the thermal decomposition of HMX at 210°C. The duration of the decomposition process is about 37000 seconds.

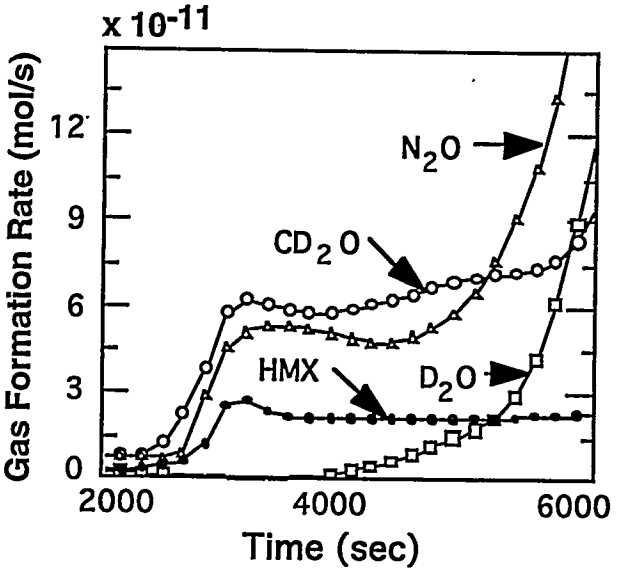

Figure 2. Gas formation rates of thermal decomposition products from HMX-d8 during the induction period and first stage of the acceleratory period.

Our previous work on the decomposition of HMX in the solid phase was conducted over a temperature range from 210° to 235°C. This work was extended to higher temperatures to investigate the qualitative behavior of HMX decomposition in the liquid phase.[8] The work covered in this paper extends the thermal decomposition measurements to lower temperatures. Since the objectives of the study are to obtain data to characterize the state of HMX under abnormal thermal conditions and to investigate the behavior of HMX during long-term aging, it is necessary to measure only the induction period and its early stages in particular, in these studies.

NEW HMX LOWER TEMPERATURE DATA

Experiments on the decomposition of HMX between 175° and 200°C have been conducted to add to the database on its decomposition behavior. The general behavior is quite similar to that observed in the previous work as can be seen from Figure 3 for the decomposition of HMX at 182°C. The ion signals representing the evolution of N_2O and CH_2O are very similar to the data collected at higher temperatures. In this case the induction period, as determined by the time at which the N_2O signal first increases, is approximately 60,000 seconds. As the N_2O signal increases, it is characterized by two different sets of rates, with the first set being less than the second. This is typical of all of the data collected in the different experiments at lower temperatures.

Comparing the induction time of N_2O to CH_2O (Figure 3) shows that the increase in the CH_2O rate of evolution lags that of N_2O by about 40,000 seconds. This behavior is similar to that observed at higher temperatures. Several other products also observed in the higher temperature experiments are dimethylnitrosamine (m/z=74), formamide (m/z=45), H_2O and CO. The temporal behaviors of these products are similar to those observed at higher temperatures.

Since there is a strong correlation between the identities and temporal behaviors of the products in the new lower temperature experiments and those of the previous higher temperature experiments, it is possible to determine the temperature dependence of the first stages of the thermal decomposition of HMX. The experimental parameters and data collected from experiments with HMX are listed in Table 1. The experiments range in temperature from 175° to 200°C (data from reference 6 is also included in Table 1). HMX samples with mean particle diameters of 150 and 600 μm were used in the experiments. The diameter of the reaction cell orifice was also varied from 10 μm to 100 μm in different experiments. Although there may be an effect due to the extent of gas product containment, which is

controlled by the orifice diameter, and particle size, these effects are small compared to the variation in the induction times and rates of reaction with temperature.

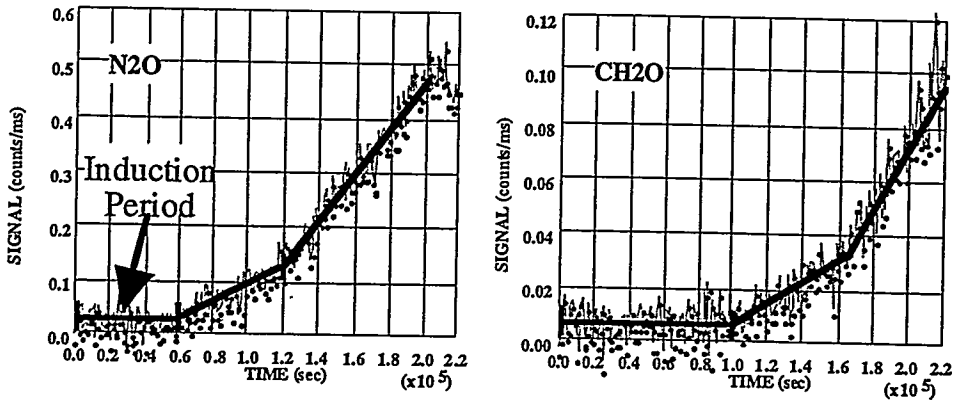

Figure 3. Ion signals representing the evolution of N_2O and CH_2O from the thermal decomposition of HMX at 182°C.

Table 1. HMX THERMAL DECOMPOSITION DATA

	Temp (°C)	Particle diameter (μm)	Orifice Diameter (μm)	Induction time (sec)	Decomposition rate constant (sec^{-1}) First	Second
1/2*	175	600	25	270000	2.85E-07	5.09E-07
3	182	600	10	64000	3.97E-07	2.30E-06
4	182	150	10	88000	4.94E-07	9.29E-07
5	182	150	100	62000		
6	200	150	100	9000	3.83E-06	8.77E-06
7	210	150	100	2600	1.30E-05	4.50E-05
8	226	150	100	800		
9	235	150	100	370		

* Experiment carried out in two parts. Sample was heated and held at 175°C for 220,000 seconds, cooled and removed from the apparatus for 5 days, and then again heated and held at 175°C for 220,000 seconds.

INDUCTION PERIOD. The temperature dependence of the induction period is shown in Figure 4. The Arrhenius parameters calculated from the data are Log(A)= 18.2 ± 0.8 and Ea = 48.2 ± 1.8 kcal/mole. The variation in the results from the three experiments conducted at 182°C using different particle sizes and different orifice diameters is shown by the data at 1/T = 0.0022 in Figure 4. The two points shown at 1/T=0.00223 sec^{-1} are two different estimates for the induction time from experiment 1/2 in which the sample heated and held at 175°C for 220000 seconds, cooled and removed from the apparatus for five days, and then reheated and held at 175°C for another 220000 seconds. The shorter induction time was taken from the data collected in the first heating cycle and the longer induction time was taken from the second heating cycle. The acceleratory phase of the decomposition was not readily apparent in the first heating cycle and the data point was based on the first apparent deviation of the N_2O signal from a constant value. The data from the second heating cycle showed a clear acceleratory period and the induction time is calculated as the sum of the time heated in the first cycle and the normal induction time measured in the second cycle.

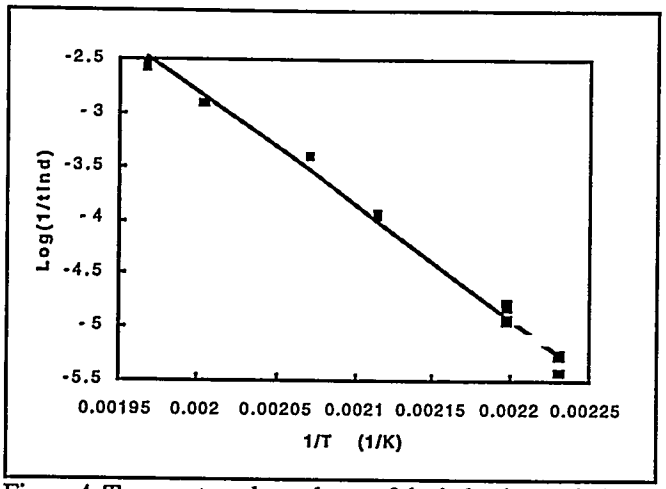

Figure 4. Temperature dependence of the induction period for the thermal decomposition of HMX.

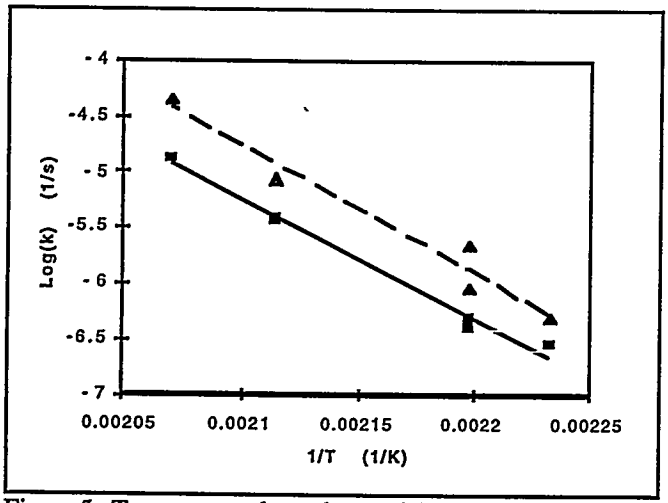

Figure 5. Temperature dependence of the 1st (squares, solid line) and 2nd (triangles, dashed line) acceleratory periods of the HMX decomposition.

The data from the experiment with the two heating cycles clearly shows that the HMX sample retains the degradation effects of prior heating. Thus, from this initial data, it appears that the effects of the degradation process that occur during the induction period are irreversible. However, further experiments need to be performed to test this more thoroughly.

ACCELERATORY PERIOD. The acceleratory period that commences at the end of the induction period is characterized by two different acceleration rates as illustrated by the N_2O data shown in Figure 3. The rate constants for these two acceleratory phases, listed in Table 1, were obtained from the corresponding weight loss data measured with the microbalance of the STMBMS apparatus. There is some variation in the rate constant calculated for the 2nd acceleratory phase due to the measurement being made on different segments of the acceleratory curve. The weight loss data were corrected for evaporation of HMX in the experiments using the reaction cell with the 100 μm diameter orifice. This correction was not necessary in the experiments using the smaller diameter orifices due to the small contribution from evaporation.

The temperature dependence of the 1st and 2nd acceleratory periods is shown in Figure 5. The Arrhenius parameters for the 1st acceleratory period are Log (A) = 17.15 ± 1.5 and Ea = 48.9 ± 3.2 kcal/mole. The Arrhenius parameters for the 2nd acceleratory period are Log (A) = 19.1 ± 3.0 and Ea = 52.1 ± 6.3 kcal/mole.

MODEL TO PREDICT LOWER TEMPERATURE BEHAVIOR FOR HMX

The data from the induction and the two acceleratory periods can be used to estimate the extent of decomposition as a function of sample temperature and time. It can also be used to estimate the extent of degradation at lower temperatures over long periods of time.

The fraction, Fr, of HMX that has decomposed up to a given point in time, t, when held at a temperature, T, is given by

$$Fr = \left[1 - Exp\left(-k_1 t_{d1}\right)\right] + \left[1 - Exp\left(-k_2 t_{d2}\right)\right]$$

where the rate constants for the 1st (k_1) and 2nd (k_2) acceleratory periods are given by

$$Log\left(k_1\right) = 1714 - \frac{10664}{T} \qquad \text{and} \qquad Log\left(k_2\right) = 1912 - \frac{11374}{T},$$

the time in each acceleratory period is given by

$$t_{d1} = Min\,(t - t_{ind})\,t_f) \qquad \text{and} \qquad t_{d2} = Min\,(t - t_{ind} - t_f, t_{fm}),$$

the induction time is given by

$$Log\,(1/t_{ind}) = 18.23 - \frac{10522}{T},$$

and t_f is the time of the transition from the first to the second acceleratory region and is given by

$$t_f = -Ln\,(1 - f_t)/k_1,$$

where f_t is the fraction of decomposition at which there is a transition from the 1st to the 2nd acceleratory phase, and t_{fm} is the time associated with the maximum fraction of decomposition, f_m, that this model is developed to predict and is given by

$$t_{fm} = -Ln\,(1 - f_m + f_t)/k_2.$$

The transition fractions used in the model are $f_t = 0.05$ and $f_m = 0.2$. The value for f_t is determined from the break points between the 1st and 2nd acceleratory periods measured in the experiments. The value of 0.2 for f_m is selected because this approximates the amount of decomposition that occurs through the acceleratory phase.

The fraction of decomposition as a function of time at several different temperatures is shown in Figure 6. For example, to achieve 5% decomposition requires the sample to be maintained at 190°C for approximately 19 hours.

HMX LONG-TERM DECOMPOSITION

The length of time predicted for the duration of the induction period and the point at which 0.01% of the sample has decomposed based on the rate constants for the first and second acceleratory periods is shown in Figure 7 for a set of temperatures varying between 20° and 130°C. The data in the table shows that if the sample is maintained at 120°C the induction period will last for 10 years before gas starts to be released in the first acceleratory period. Whereas, if the reaction kinetics that controls the decomposition was based on the reactant rates that characterize the two acceleratory periods, then the sample only needs to be maintained between 80° and 90°C to undergo 0.01% decomposition in ten years. This illustrates the importance of the process that occurs in the induction period in contributing to the long-term stability of HMX. For example, at 70°C the induction period would last 85,000 years, whereas, decomposition controlled by solely the acceleratory period reactions would occur over 200 to 300 years.

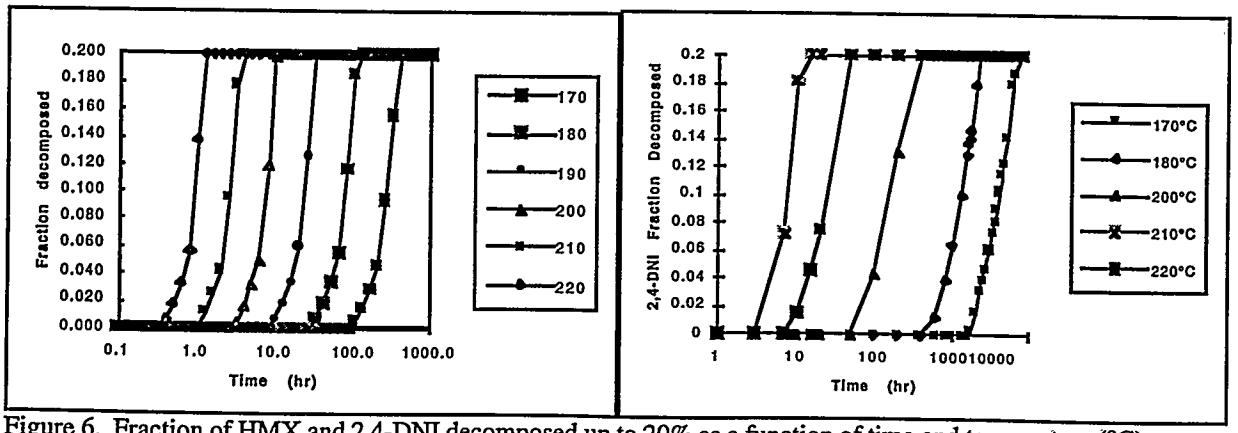

Figure 6. Fraction of HMX and 2,4-DNI decomposed up to 20% as a function of time and temperature (°C).

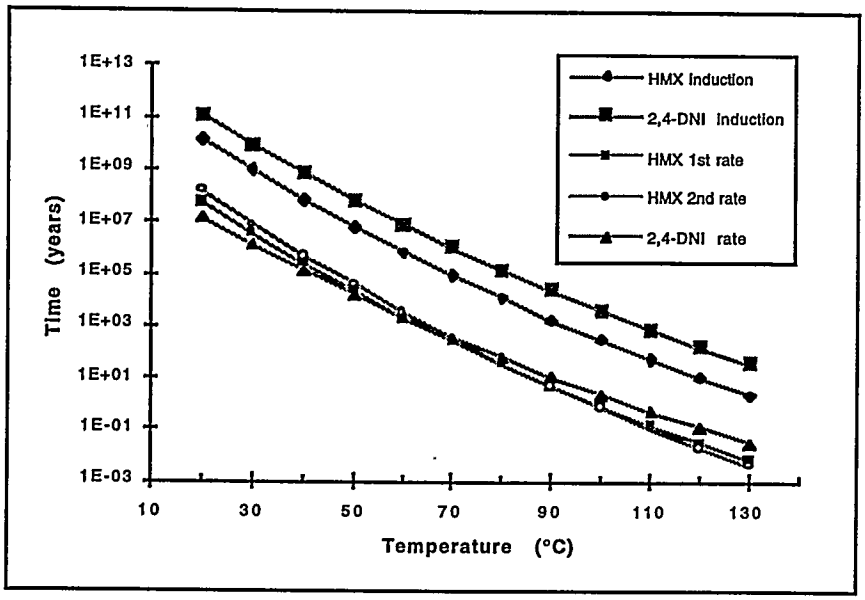

Figure 7. Modeled thermal stability curves of the induction period and constant rate periods for HMX and 2,4-DNI.

Clearly, this data suggests that under normal storage conditions (< 70°C) HMX should be stable over the lifetime of any component in which it is used, based on these decomposition measurements of pure HMX. However, there are several other points that should be considered regarding the decomposition of HMX. First, it is possible that reactions may occur between HMX and other materials that may come in contact with the particle surface. This may occur at lower temperatures than the decomposition of HMX by itself. These interactions may present a long-term aging issue. Second, during the induction period HMX must undergo some significant changes. These changes may be chemical, physical or both. It is unlikely that they would affect the combustion or detonation behavior of these materials, since no significant change in the energy content of the material is observed. However, these changes may affect the thermal or impact sensitivity if they cause significant changes in the way "hot spots" are formed in the material. Third, the decomposition processes that we have studied above 210°C also occur at lower temperature. Thus, it is reasonable to assume that the details of the reaction processes that we have observed at higher temperatures also occur at lower temperatures (reaction in the lower temperature ß-HMX may differ from the higher temperature ∂-HMX measured in these studies). This process which was observed in the solid phase decomposition of RDX and HMX is the formation of the mononitroso analogue of the parent compound. From our previous data we believe that the mononitroso analogue is formed within the solid lattice. The conversion of HMX to its mononitroso analogue occurs through scission of the N-NO_2 bond and reaction of the NO within the surrounding "lattice cage". This is consistent with the results of our isotopic crossover experiments using ^{15}N labeled HMX, which showed that 75% of the mononitroso analogue of HMX formed in the experiment did not participate in isotopic scrambling. It is also consistent with the activation energy of 48.2 ± 1.8 kcal/mole for the induction period measured in this study which is very close to the N-NO_2 bond energy of approximately 45 kcal/mole. From our thermal decomposition studies of the mononitroso analogue of RDX we have found that it is significantly less stable than RDX and its main decomposition products are N_2O and CH_2O. This is quite consistent with the products observed in the decomposition of HMX in this study. Thus, from these results, it appears that the process that occurs in the solid phase at low temperature may also be scission of the N-NO_2 bond, reaction of the NO_2 within a "lattice cage" to form the mononitroso analogue of HMX, decomposition of the mononitroso HMX within the HMX lattice to form gaseous products that are retained in bubbles or diffuse into the surrounding lattice. These products may affect the sensitivity of HMX significantly.

2,4-DNI LOW TEMPERATURE THERMAL DECOMPOSITION PROCESS

CONDENSED-PHASE THERMAL DECOMPOSITION. 2,4-DNI is being evaluated as a potentially less-sensitive substitute for HMX in composite explosive formulations.[9] We have characterized the evaporation of 2,4-DNI[10] and now are characterizing its thermal decomposition. Similar to HMX, 2,4-DNI liquefies between approximately 265° and 270°C. The temperature range evaluated in this study is between 200° and 247°C. In a typical 2,4-DNI decomposition experiment, the main decomposition products are NO, CO_2, H_2O, HNCO, N_2, CO and a nonvolatile residue. Minor gaseous products with similar temporal behaviors include HCN, C_2N_2 and NO_2. The behavior during the early stages of 2,4-DNI thermal decomposition process will be presented in this paper. A detailed description of the entire process will be presented in a later paper.

EARLY THERMAL DECOMPOSITION CHARACTERISTICS. The experimental data from the condensed-phase thermal decomposition experiments are shown in Table 2. The early stages of 2,4-DNI decomposition are illustrated in the data shown in Figure 8 for decomposition at 235°C. The temporal behavior of the ion signals representing the major gaseous decomposition products HNCO (*m/z*=43), H_2O (*m/z*=18) and CO_2 (*m/z*=44), as well as a residual impurity from synthesis, 4-nitroimidazole (4-NI; *m/z*=113), are typical of all the condensed-phase decomposition experiments. The initial decomposition is characterized by the five following events: 1) An immediate evolution of contaminants and impurities as isothermal temperature is being achieved. In this case, the isothermal temperature of 235°C is achieved at approximately 2200 seconds. 2) Simultaneous with 4-NI evolution is the desorption of H_2O from the 2,4-DNI. 3) An early decomposition occurs from about the onset of the isothermal temperature to approximately 4000 seconds. 4) An induction period ensues that is determined from the onset of isothermal temperature to the time that an increase in the HNCO is observed after the early decomposition is complete (in this case, at approximately 9000 seconds). 5) Then following the induction period, the HNCO signal shows an accelerating rate of evolution. This accelerating rate can be approximated by a linear rate of increase up to approximately 15000 seconds. After this approximated linear rate of increase of HNCO, other product signals, such as H_2O and CO_2, show an accelerating rate of increase. The portion of the decomposition up to 15000 seconds comprises the events utilized to characterize the initial decomposition behavior of 2,4-DNI.

Table 2. 2,4-DNI THERMAL DECOMPOSITION DATA

Experiment Number	Temp (C)	Orifice Diameter (μm)	Induction time (sec)	rate constant[a] (sec^{-1})
1	200.4	10	212000	b
2	209.8	25	70000	b
3	210.5	25	68000	7.64E-07
4	225.4	25	17100	2.59E-06
5	225.0	25	16000	2.85E-06
6	235.2	25	6850	4.22E-06
7	235.2	25	6600	6.56E-06
8	246.9	25	2250	2.05E-05

[a] Global rate constants determined from weight-loss curves of the STMBMS that have been corrected for evaporation.

[b] Weight-loss data not corrected at this time. Fraction of 2,4-DNI evaporation at this temperature has not been evaluated.

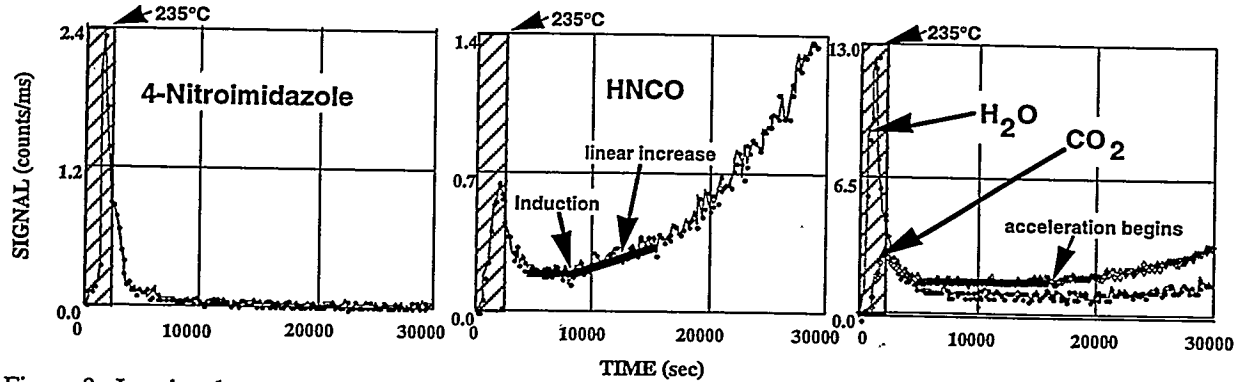

Figure 8. Ion signals representing the early evolution of the products HNCO, C_2N_2, H_2O, CO_2 and the impurity 4-nitroimidazole (4-NI) from the thermal decomposition of 2,4-DNI at 235°C (reached at about 2200 seconds).

The early decomposition observed near the onset of the isothermal temperature is due to many factors such as the presence of impurities and the condition of the crystal lattice. Imperfections within the lattice caused by the presence of contaminants, including adsorbed and occluded H_2O molecules, can initiate the decomposition of 2,4-DNI molecules not stabilized by the lattice. Separate studies of 4-NI thermal decomposition show that under similar experimental conditions, 4-NI undergoes substantial evaporation with little decomposition. However, the

dinitroimidazole isomers of 1,4-DNI and 4,5-DNI decompose and melt at temperatures below 200°C and the temporal behavior of ion signals associated with these dinitroimidazole isomer decomposition products indicate their presence during the early decomposition period. However, these contaminants are typically less than 1%-2% (w/w) of the 2,4-DNI sample. The major contributor to the early decomposition is H_2O. The end of the early decomposition stage, shown in Figure 8, coincides with the decrease in the H_2O signal at about 4000 seconds. The H_2O signal observed during the initial stages of 2,4-DNI degradation is suspected to originate from adsorbed and occluded H_2O, not from H_2O as a thermal reaction product.

EFFECT OF H_2O ON 2,4-DNI THERMAL DECOMPOSITION. The effect of H_2O on 2,4-DNI decomposition is important to understand since it has a measurable affect on the early decomposition process and may affect the thermal stability of a system that contains 2,4-DNI. To determine if H_2O was a factor in the early decomposition, the 235°C isothermal experiment was repeated with a 1.5 hour hold at 120°C to minimize the amount of any adsorbed H_2O. The resulting H_2O signal, shown in Figure 9, shows a strong evolution during the 125°C hold, supporting the presence of adsorbed H_2O since the 2,4-DNI is not undergoing major decomposition at this temperature. As 235°C is reached (~6000 seconds), the H_2O signal again increases as remaining H_2O desorbs from the sample, indicating that water is still present with the material. The peak widths of the decomposition products HNCO and CO_2 are narrow, relative to the corresponding peak widths shown in Figure 9, suggesting a lesser amount of these products has evolved. Similar to the product evolution shown in Figure 8, the early HNCO and CO_2 signal decrease with the decrease in the H_2O signal. This again suggests that the early decomposition is correlated to the presence of H_2O. The H_2O will readily react with the probable 2,4-DNI decomposition intermediates that form during the induction period. Specifically, we have deduced a general thermal decomposition mechanism for 2,4-DNI (Figure 10), based on decomposition studies conducted in this lab using 2,4-DNI isotopomers, that involves the formation of a cyanate intermediate. The intermediate is formed after a nitro-nitrite rearrangement occurs to form an oxy radical that, in turn, rearranges to form a cyanate functionality (R-C=N=O). Cyanates readily react with H_2O to produce CO_2. Later in the reaction the H_2O is a product of decomposition, being formed by hydrogen abstraction of a nitro group to form a hydroxy radical that further abstracts hydrogen to form H_2O. After the impurities are depleted, including the desorbed and occluded H_2O, the early decomposition event ceases and the continuation of the normal induction period of 2,4-DNI is observed. Based on our initial evaluations, the induction period does not appear to be significantly changed by the amount of the early decomposition that occurs, being approximately 7500 seconds for the 235°C isothermal experiments represented in Figures 8 and 9. Further experiments to evaluate the effect of H_2O on the early decomposition of 2,4-DNI are presently being conducted.

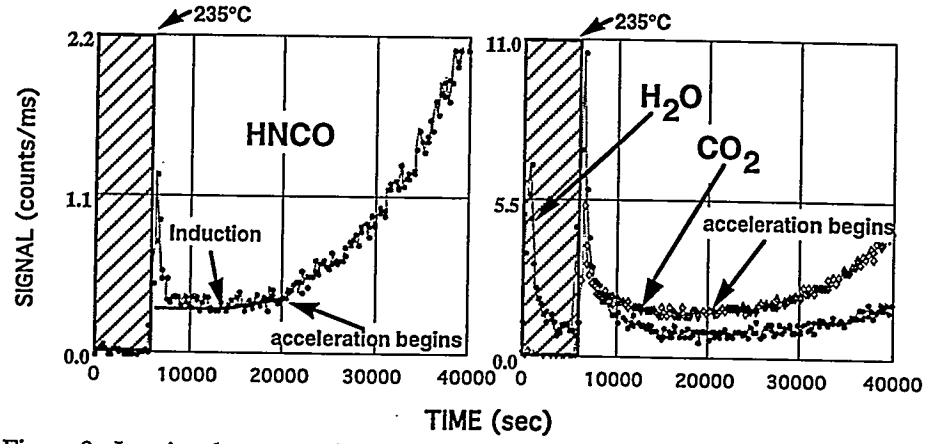

Figure 9. Ion signals representing the early evolution of H_2O, CO_2 and HNCO during the thermal decomposition of 2,4-DNI with an isothermal hold at 120°C to ~5000 seconds and a ramp to an isothermal hold at 235°C (reached at about 6000 seconds).

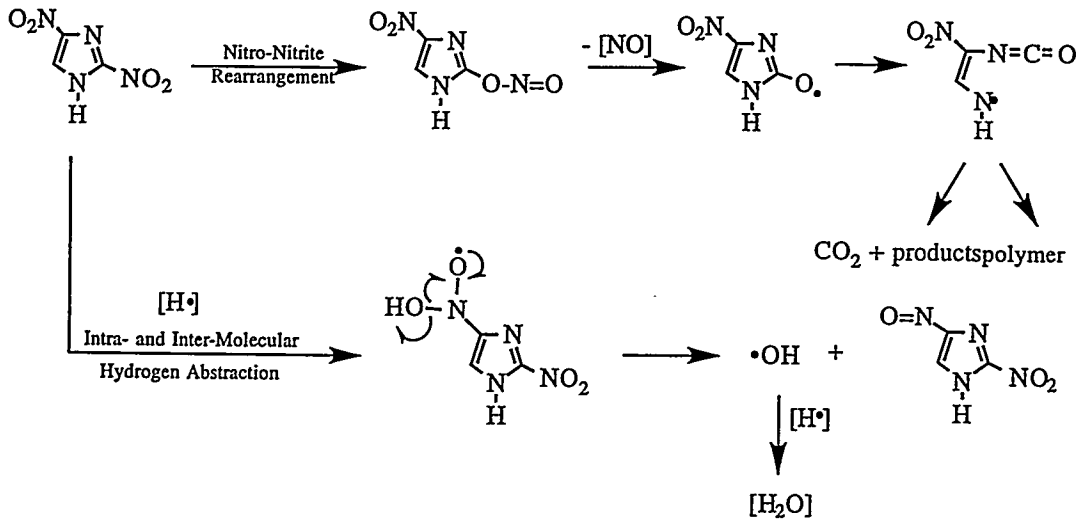

Figure 10. Initial mechanisms for 2,4-DNI condensed-phase thermal decomposition.

EARLY DECOMPOSITION KINETICS. Assuming the early decomposition does not affect the normal thermal degradation of that for pure 2,4-DNI, then the induction and initial acceleratory periods measured with the product HNCO represents the decomposition behavior as a function of temperature. The time of the induction period is measured from the onset of the isothermal temperature to the time the HNCO signal begins increasing into the initial acceleratory period. The rate constants (Table 2) for the initial acceleratory periods between 225° and 247°C are obtained by correcting the weight-loss data for 2,4-DNI evaporation. The temperature dependence of these two periods are shown in Figure 11. The Arrhenius parameters for the induction period are [Log(A) = 16.3 ± 0.3 and Ea = 46.9 ± 0.7 kcal/mole] and for the initial accelerating period are [Log (A) = 13.4 ± 1.7 and Ea = 42.7 ± 3.9 kcal/mole]. Using the same model as expressed for HMX decomposition with the above Arrhenius parameters, only one transition fraction, and setting $f_m = 0.2$, the time for 0.01% decomposition of 2,4-DNI can be determined as that of HMX and is included with the HMX data shown in Figures 6 and 7. Further studies will verify if these kinetics do indeed approximate pure 2,4-DNI thermal decomposition.

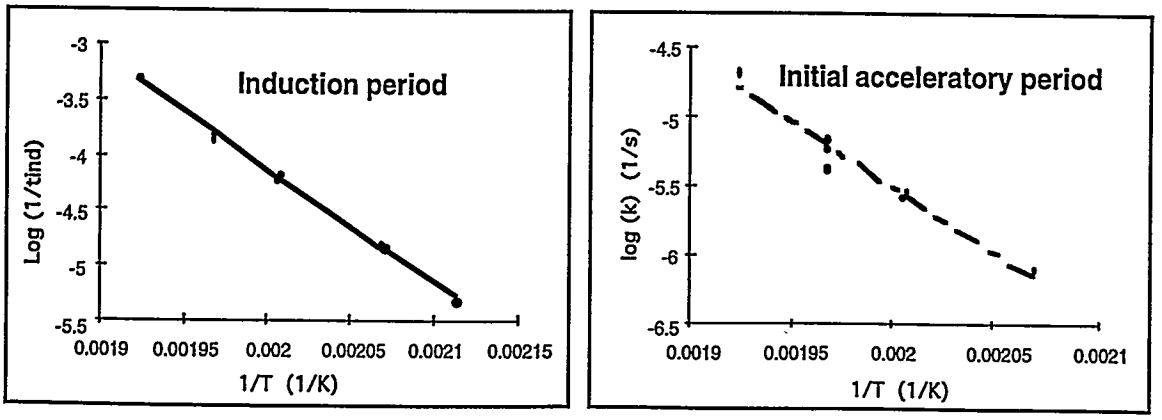

Figure 11. Arrhenius parameters for the induction period and the initial acceleratory period of 2,4-DNI.

Conclusions

HMX

The decomposition of HMX between 175° and 210°C exhibits the same behavior as HMX above 210°C. The identity and temporal behavior of the products formed in the lower and higher temperature ranges are similar. Thus, the results of mechanistic studies conducted at the higher temperature range are applicable to the reactions at lower temperatures.

The early stages of the decomposition of HMX can be divided into three segments, an induction period followed by two acceleratory periods. The end of the induction period is characterized by the increase in the rate of N_2O evolving from the sample. The increase in the rate of evolution of CH_2O always lags that of N_2O, suggesting that CH_2O is initially retained in the HMX lattice. Other products such as formamide and dimethylnitrosamine are also observed.

The A-factors and activation energies for the induction period and two acceleratory periods are (Log(A)= 18.2 ± 0.8, Ea = 48.2 ± 1.8 kcal/mole), (Log (A) = 17.15 ± 1.5 and Ea = 48.9 ± 3.2 kcal/mole), (Log (A) = 19.1 ± 3.0 and Ea = 52.1 ± 6.3 kcal/mole), respectively. These activation energies are similar to N-NO_2 bond energy in HMX.

Using the Arrhenius parameters determined from the measurements, estimates of the length of time that an HMX containing sample must be held at a given temperature to achieve a desired fraction of decomposition can be determined. This data can be used for preparing samples for testing the effects of thermal degradation on sensitivity and burn rates.

Extrapolating the HMX thermal decomposition results to lower temperatures shows that the degradation is not extensive at the upper temperature limit of the normal stockpile to target sequence, 70°C. However, raising the temperature to 120°C would have a significant effect on the material if it behaves as measured in the present experiments. If for some reason the stability attributed to the induction period were lost and the rate of reaction were controlled by the reactions occurring in the acceleratory phase, then raising the temperature to 85°C would cause significant changes in the material.

The similarity of the results of the lower temperature experiments carried out in this study to our previous mechanistic studies of HMX and RDX at higher temperature allows us to suggest that the following process probably occurs in the early stages of the solid phase decomposition of HMX: scission of the N-NO_2 bond, reaction of the NO_2 within a "lattice cage" to form the mononitroso analogue of HMX and decomposition of the mononitroso HMX within the HMX lattice to form gaseous products that are retained in bubbles or diffuse into the surrounding lattice.

Further studies are needed to accurately characterize the effects of particle size, gas containment, and cycling the sample temperature on the thermal decomposition process. However, several experiments conducted in the present study, in which these parameters were varied, indicate that these effects are secondary compared to the variation due to temperature.

2,4-DNI

The 2,4-DNI early thermal decomposition process between 200° and 247°C first undergoes an early decomposition attributed to the presence of impurities remaining from the synthesis and from adsorbed and occluded H_2O in the 2,4-DNI crystal lattice. Upon depletion of the impurities, an apparent induction period is observed that is defined to be from the onset of the isothermal temperature to time of the increase of the HNCO signal. The induction period is followed by an initial acceleratory period.

The presence of H_2O has an effect on early 2,4-DNI thermal decomposition. The increase of the early decomposition product signals, namely CO_2 and HNCO, occurs shortly after the increase of the adsorbed H_2O signal occurs. These signals then decrease with the decreasing H_2O signal. Decreasing the amount of adsorbed water gives an apparent reduction in the amount of the early decomposition products such as CO_2 and HNCO. The presence of H_2O impurity does not significantly affect the induction time at 235°C. Further studies are being conducted to evaluate the effect of H_2O in further detail.

The Arrhenius parameters for the induction period are Log(A) = 16.3 ± 0.3 and Ea = 46.9 ± 0.7 kcal/mole and for the initial accelerating period are Log (A) = 13.4 ± 1.7 and Ea = 42.7 ± 3.9 kcal/mole. These parameters are based on the assumption that the early decomposition does not affect the kinetics of pure 2,4-DNI thermal decomposition.

The methods used to evaluate the thermal decomposition mechanisms and kinetics of HMX can be used to comparatively evaluate new energetic materials. The HMX thermal decomposition model is applied to 2,4-DNI decomposition. Verification of the 2,4-DNI Arrhenius parameters that are used in the model are presently being verified with further studies.

COMPARISON OF HMX AND 2,4-DNI DECOMPOSITION

The physical processes responsible for controlling the thermal decomposition of HMX and 24DNI are similar although the chemical reactions that lead to these processes are clearly different. In both materials chemical reactions occur within the solid particles that lead to weakening of the crystal structure. For the case of HMX, the results indicate that it decomposes through the mononitroso intermediate to form CH_2O, N_2O and other gaseous products. The formaldehyde diffuses through the surrounding lattice, weakening it, and leading to liquefaction. For the case of 2,4-DNI, the presence of water within the lattice, either occluded from the synthesis or formed in the thermal decomposition, promotes the decomposition of 2,4-DNI and weakening of the surrounding crystal lattice.

ACKNOWLEDGMENTS

The authors wish to thank D.M. Puckett for assistance in collecting the mass spectrometry data.

REFERENCES

1. J. Maienschein, private communication.
2. R. Behrens, Jr.; *Rev. Sci. Instrum.* **58**, 451-461, 1987.
3. a) R. Behrens, Jr.; *Int. J. Chem. Kin.* **22**, 135-157, 1990. b) R. Behrens, Jr.; *Int. J. Chem. Kin.* **22**, 159-173, 1990.
4. R. Behrens, Jr. and S. Bulusu; *J. Phys. Chem.* **96**, 8877-8891, 1992.
5. R. Behrens, Jr. and S. Bulusu; *J. Phys. Chem.* **96**, 8891-8897, 1992.
6. R. Behrens, Jr.; *J. Phys. Chem.* **94**, 6706-6718, 1990.
7. R. Behrens, Jr.; *J. Phys. Chem.* **95**, 5838-5845, 1991.
8. R. Behrens, Jr. and S. Bulusu; *Mat. Res. Soc. Symp. Proc.*, **296**, p. 18-24, 1993.
9. K. Jayasuriya, R. Damauarapu, R.L. Simpson, C.L. Coon, and M.D. Coburn; "2,4-Dinitroimidazole: A Practical Insensitive High Explosive?" Lawrence Livermore National Laboratory, UCRL-ID-11133G4, March 12, 1993.
10. L. Minier, R. Behrens, Jr. and S. Bulusu; *J. Mass Spec.* In press.